NANO LETTERS

2001
Vol. 1, No. 5
245−251

Modulable Nanometer-Scale Surface Architecture Using Spin-Coating on an Adsorbed Collagen Layer

Christine C. Dupont-Gillain and Paul G. Rouxhet*

Unité de Chimie des Interfaces, Université Catholique de Louvain, 1348 Louvain-la-Neuve, Belgium

Received January 11, 2001 *(Revised Manuscript Received March 14, 2001)*

ABSTRACT

A strategy was developed to create a modulable polymer surface architecture (topography, chemical composition) at the nanometer scale. Therefore, collagen was first adsorbed on a poly(methyl methacrylate) (PMMA) substrate and dried at high or low rate to produce continuous or discontinuous layers, respectively. Solutions of PMMA in chlorobenzene were then spin-coated on top of these collagen layers. The obtained surfaces were investigated using atomic force microscopy and X-ray photoelectron spectroscopy. Spin-coating with pure chlorobenzene on the continuous collagen layer produced pits in the PMMA substrate through the collagen layer; spin-coating with PMMA solutions of increasing concentrations progressively led to the formation of a surface covered by particles made of PMMA and collagen, resulting from a combination of dissolution of PMMA from the substrate and deposition of PMMA from the solution. Spin-coating with pure chlorobenzene on the discontinuous collagen layer led to dissolution of PMMA and to its redeposition on the collagen pattern, which served as a template. This provided a surface entirely composed of PMMA, with cavities in the range of 0.1–1 μm diameter and 50–250 nm depth. In this case, the surface relief was independent of the PMMA concentration of the spin-coated solution, the substrate PMMA dissolution and redeposition being the dominant processes.

1. Introduction. The control of surface roughness is of particular relevance in fields as diverse as adhesion, wetting, tribology, optics, and biomaterial design. Different methods have been developed, allowing the creation of surface topography at the micrometer scale. These include particle blasting,[1] laser ablation,[2] settling of microspheres,[3] methods based on photolithography,[4−7] or on microcontact printing.[8] More recently, the interest has also been focused on the production of surface patterns at the nanometer scale, using phase separation[9] or nanolithography[10] in self-assembled monolayers, electron beam lithography,[11] imprint lithography,[12] or colloidal lithography.[13] These topographical changes at the micro- or the nanometer scale are, in most cases and to a lesser or a greater extent, accompanied by chemical modifications of the surface. Curtis and Wilkinson recently reviewed the reactions of mammalian cells to nanotopography.[14] They concluded that many questions remained unanswered and, in that view, the design of new nanostructured surfaces with controlled chemistry is an important challenge.

Crystalline protein monolayers originating from the surface of bacteria, so-called S-layers, were suggested to be used as nanotemplates or nanoresists.[15] They have been used to control the etching of a thin metal coating, producing a periodic array of 10-nanometer holes, in which the underlying graphite substrate was exposed.[16] The surface organization of adsorbed proteins varies according to the physicochemical properties of the substrate and the adsorption parameters, thus opening the way to a large variety of nanostructures. Collagen adsorbed on mica was shown to form large fibrils at high concentration and pH, and a fine meshwork at low concentration and pH.[17] Collagen presented different nanoscale organizations on different polymers;[18] this was also observed for a mussel adhesive protein.[19] Changes in substrate surface properties combined with drying were shown to affect the surface organization as well, with the production of particular patterns in some cases.[20−24] Controlling the rate of drying after adsorption of collagen on poly(methyl methacrylate) (PMMA) allowed varying the surface organization, from a continuous to a discontinuous adsorbed layer at high and low drying rates, respectively.[25]

Spin-coating of polymer solutions is commonly used to planarize surfaces, i.e., to reduce or eliminate topographic features. Many theoretical and experimental studies have led to the determination of a range of parameters favoring planarization. The most important are high film thickness, low viscosity solution, low molar mass polymer, low volatility solvent, and low spinning speed. The geometry and the location of the surface asperities to be planarized are determinant as well.[26−32]

In this paper, we present an original strategy to create a modulable polymer surface architecture at the nanometer

* Corresponding author. E-mail: rouxhet@cifa.ucl.ac.be.

10.1021/nl010002x CCC: $20.00
Published on Web 04/13/2001

scale. The method involves adsorption of macromolecules on a polymer surface followed by spin-coating of an appropriate solution. It takes advantage of the surface organization of the adsorbate to further create a chemically homogeneous but nanometer-scale-tailored polymer surface. Spin-coating is used, not for planarization, but to exacerbate a previously designed surface topography. The polymer used both as a substrate and for spin-coating is poly(methyl methacrylate) (PMMA), an amorphous polymer widely used to elaborate biomaterials such as contact lenses and teeth and bone cements.[33] The adsorbate is collagen, an extracellular matrix protein.

2. Materials and Methods. *2.1. Sample Preparation.* Poly(methyl methacrylate) (PMMA) (Aldrich, Milwaukee, WI; $M_w = 996\,000$) plates were obtained by compression molding between two glass plates at 240 °C. For the sake of uniformity, they were all spin-coated (time = 60 s, speed = 5000 rpm, acceleration = 20 000 rpm/s, temperature = 20 °C) with a 10% (w/w) solution of the same PMMA in chlorobenzene (VEL, Leuven, Belgium).

Collagen (type I from calf skin, Boehringer-Mannheim, Mannheim, Germany) was received as an aqueous solution (3 mg/mL at pH 3.0). It was diluted in phosphate-buffered saline solution (PBS) (137 mM NaCl (Merck, Leuven, Belgium), 6.44 mM KH_2PO_4 (VEL), 2.7 mM KCl (Merck), and 8 mM Na_2HPO_4 (VEL)) to a concentration of 7 μg/mL. Adsorption of collagen was performed as follows: a circular PMMA sample (radius = 6 mm) was placed in a well of a tissue culture plate (Falcon, Franklin Lakes, NJ); 2 mL of the collagen solution were added and the collagen was allowed to adsorb during 2 h at 37 °C. The sample was then rinsed three times, without removal from the solution, by pumping 1.8 mL of the liquid, adding 1.8 mL of water (HPLC grade produced by a MilliQ plus system from Millipore, Molsheim, France, hereafter referred to as MilliQ), and gently agitating for 5 min. After rinsing, the samples were removed from the wells and two different drying procedures were applied. A fast-drying (FD) procedure was performed by flushing the samples with a nitrogen flow; the samples were then stored in a desiccator containing P_2O_5. A slow-drying (SD) procedure was performed by placing the wet samples for a period of 2−3 days in a closed vessel containing a saturated solution of Na_2CO_3 (VEL), which maintained a relative humidity of about 95%.

Solutions of PMMA in chlorobenzene were prepared at the following concentrations: 0.0, 0.2, 0.5, 1.0, and 2.0 g/L. 100 μL of these solutions were spin-coated (time = 60 s, speed = 5000 rpm, acceleration = 20 000 rpm/s, temperature = 20 °C) on the PMMA samples on which collagen had been previously adsorbed and dried.

To evaluate the thickness of PMMA films produced by spin-coating, the same solutions and parameters were used with an inert and smooth solid surface consisting of 1 cm^2 pieces of silicon wafers (Wacker-Chemitronic, Burghausen, Germany).

2.2. Surface Characterization. XPS spectra were recorded using a SSX-100 spectrometer (model 206 from Surface Science Instruments, Mountain View, CA) equipped with a monochromatized aluminum anode (10 kV, 12 mA). The angle between the normal to the sample surface and the direction of photoelectron collection was 55°. The order of peak analysis was: survey scan, C_{1s}, O_{1s}, and N_{1s} (except for the samples prepared with silicon wafers for which the order was: survey scan, C_{1s}, O_{1s}, and Si_{2p}). Intensity ratios were converted into molar concentration ratios by using the sensitivity factors proposed by the manufacturer (Scoffield photoemission cross-sections, variation of the electron mean free path according to the 0.7th power of the kinetic energy, constant transmission function).

AFM images (5 × 5 μm^2) were obtained, in ambient conditions, in the contact mode using a commercial microscope (Nanoscope III, Digital Instruments, Santa Barbara, CA) equipped with Si_3N_4 triangular levers (Park Scientific Instruments, Sunnyvale, CA; typical radius of curvature = 20 nm, typical spring constant = 0.01 or 0.03 N/m). The scan rate was 1 Hz. The applied force was minimized before each image acquisition.

The thickness of the PMMA layers obtained by spin-coating on silicon wafers was also evaluated using AFM. For this purpose, a 300 × 300 nm^2 area was first imaged at high loading force; a larger image was then acquired, allowing to measure the depth of the previously damaged area.

Table 1. O/C and N/C Molar Concentration Ratios Determined by XPS on PMMA Disks Conditioned with Collagen and Subsequently Submitted to PMMA Spin-Coating

collagen conditioning		spin-coating	molar ratio	
concn (μg/mL)	drying	[PMMA] (g/L)	O/C	N/C
0[a]	FD	none	0.41	<0.005
0[a]	FD	0.0	0.42	<0.005
0[a]	FD	2.0	0.41	<0.005
7	FD	none	0.38[c]	0.123[b]
7	FD	0.0	0.37[b]	0.113[b]
7	FD	0.2	0.39[b]	0.073[b]
7	FD	1.0	0.41[b]	0.013[b]
7	FD	2.0	0.40[b]	0.010[b]
7	SD	none	0.38[b]	0.079[b]
7	SD	0.0	0.45[b]	<0.005
7	SD	0.2	0.39[b]	<0.005
7	SD	0.5	0.37[b]	<0.005
7	SD	1.0	0.40[b]	<0.005
7	SD	2.0	0.39[b]	<0.005

[a] Conditioning with pure PBS. [b] Mean value of at least two independent measurements; the range of the data was not larger than 0.04. [c] Mean value of three independent measurements; range of 0.07.

3. Results. The O/C and N/C molar concentration ratios determined by XPS are presented in Table 1. The O_{1s} and C_{1s} spectra recorded on the three samples prepared without collagen were similar to those presented in the literature[34] and the O/C ratios were close to the value of 0.40 expected from the stoichiometry of PMMA. Adsorption of collagen led to N/C ratios of 0.12 and 0.08 at high and low drying rates, respectively, while the O/C ratios were not appreciably affected compared to the O/C ratios of samples conditioned with PBS. The C_{1s} and O_{1s} peaks were a combination of

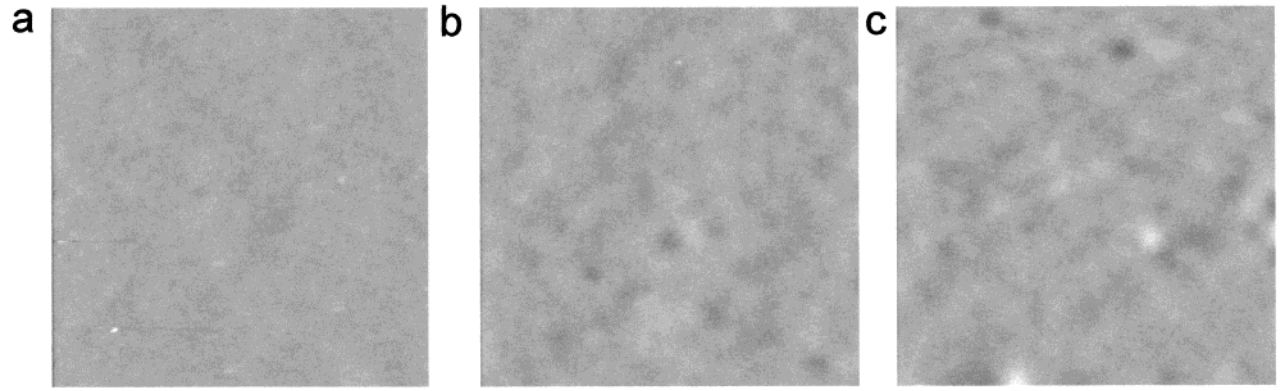

Figure 1. AFM images (size = 5 × 5 μm^2; *z*-range = 10 nm) of PMMA substrate after PBS conditioning (a) and subsequent spin-coating with pure chlorobenzene (b) or with a 2.0 g/L PMMA solution (c).

those of PMMA and collagen, the PMMA contribution being more important at low compared to high drying rate.

The surface composition of samples prepared by collagen adsorption, fast drying and subsequent spin-coating was dependent on the concentration of the spin-coated PMMA solutions: the N/C ratio was not significantly affected by spin-coating the solvent; it was approximately reduced by half at a PMMA concentration of 0.2 g/L, and it dropped by a factor of 10 at concentrations of 1.0 and 2.0 g/L. The C_{1s} and O_{1s} spectra changed progressively, with a decrease of the collagen contribution as the PMMA concentration increased. Spin-coating with PMMA solutions and even with the solvent alone on the samples dried at low rate after collagen adsorption provoked the disappearance of the nitrogen signal. The C_{1s} and O_{1s} spectra were similar to those of pure PMMA, even when the pure solvent was spin-coated.

The thickness of the layer obtained by spin-coating with PMMA solutions of concentrations of 2.0, 1.0 and 0.5 g/L on silicon wafers was estimated, using AFM, to be respectively about 5, 2, and 1 nm. At a concentration of 0.2 g/L, the layer was no longer continuous. The XPS data were modeled in order to confirm these results. The Si_{2p} peak was decomposed into contributions of oxidized (Si_{ox}) and elemental (Si_{el}) forms, and the thickness of the oxide layer present at the surface of silicon was estimated, using the Si_{ox}/Si_{el} ratio, to be 2.0 nm (parameters used: concentrations $C_{Si,Si_{el}} = 85.7$ mmol/cm^3, $C_{Si,Si_{ox}} = 18.7$ mmol/cm^3; inelastic electron mean free paths $\lambda_{Si,Si_{el}} = \lambda_{Si,Si_{ox}} = 2.9$ nm[35]). The thickness of the PMMA layer was then evaluated using the ratio of concentrations of carbon involved in ester bonds and of elemental silicon, considering a continuous layer of PMMA over a 2.0 nm thick silicon oxide layer, itself covering a silicon substrate (additional parameters used: concentration $C_{O-C=O,PMMA} = 11.9$ mmol/cm^3; inelastic electron mean free paths $\lambda_{C,PMMA} = 3.25$ nm[36] and $\lambda_{Si,PMMA} = 2.9$ nm). The PMMA thickness was found equal to 3.4, 1.4, 0.8, and 0.5 nm at respective concentrations of 2.0, 1.0, 0.5, and 0.2 g/L, which was in the same range as the thicknesses measured using AFM.

AFM images obtained on the three samples prepared without collagen (Table 1) are presented in Figure 1. When no spin-coating was performed following conditioning with PBS, the PMMA surface was very smooth (rms roughness (R_{rms}) = 0.4 nm on 5 × 5 μm^2 areas) and defect-free. After spin-coating with the pure solvent or a 2.0 g/L PMMA solution, the surface was slightly rougher (R_{rms} = 1.1 nm on 5 × 5 μm^2 areas) and presented some holes or bumps.

Images acquired on samples dried at high rates after collagen adsorption, before and after spin-coating with PMMA solutions of increasing concentrations, are shown in Figure 2, with cross-sections showing the characteristics of the relief obtained. The adsorbed collagen layer was homogeneous and smooth (R_{rms} = 0.8 nm on 5 × 5 μm^2 areas) as shown by image *a*, which has the same *z*-range as the images of Figure 1. Spin-coating with pure chlorobenzene on top of this layer provoked the appearance of a rather regular array of holes, as illustrated by image *b*. Quantification of the hole dimensions made on three independent samples, with three images each, gave a diameter of the order of 100−400 nm, a depth of the order of 10−50 nm, and a surface occupancy of about 23%. After spin-coating with a 2.0 g/L PMMA solution, the surface relief was much more pronounced and had a different character, as shown by image *f*. No clear baseline could be identified; the surface seemed to be covered by particles of a height of the order of 30−80 nm and a width of the order of 100 nm, which tended to aggregate and occupied about 63% of the surface (dimensions obtained by analysis of three independent samples, with three images each). The situations at 0.2 g/L (image c), at 0.5 g/L (image d), and at 1.0 g/L (image e) were intermediate between those at 0.0 and 2.0 g/L.

AFM images and cross-sections obtained on samples dried at low rates after collagen adsorption, before and after spin-coating with PMMA solutions of increasing concentrations, are presented in Figure 3. The adsorbed collagen layer was discontinuous, as illustrated by image a, which has the same *z*-range as the images of Figures 1 and 2a. It showed holes with a diameter of the order of 100−1000 nm and rims with a thickness of the order of 3−12 nm. Spin-coating with PMMA solutions of concentrations from 0.0 to 2.0 g/L led to a surface architecture independent of the PMMA concentration; it showed cavities with a diameter of the order of 100−1500 nm and a depth of the order of 50− 250 nm.

The topographies of the surfaces may be compared at different length scales, using 2D power spectral density analysis of the fast Fourier transform of the AFM images.[37]

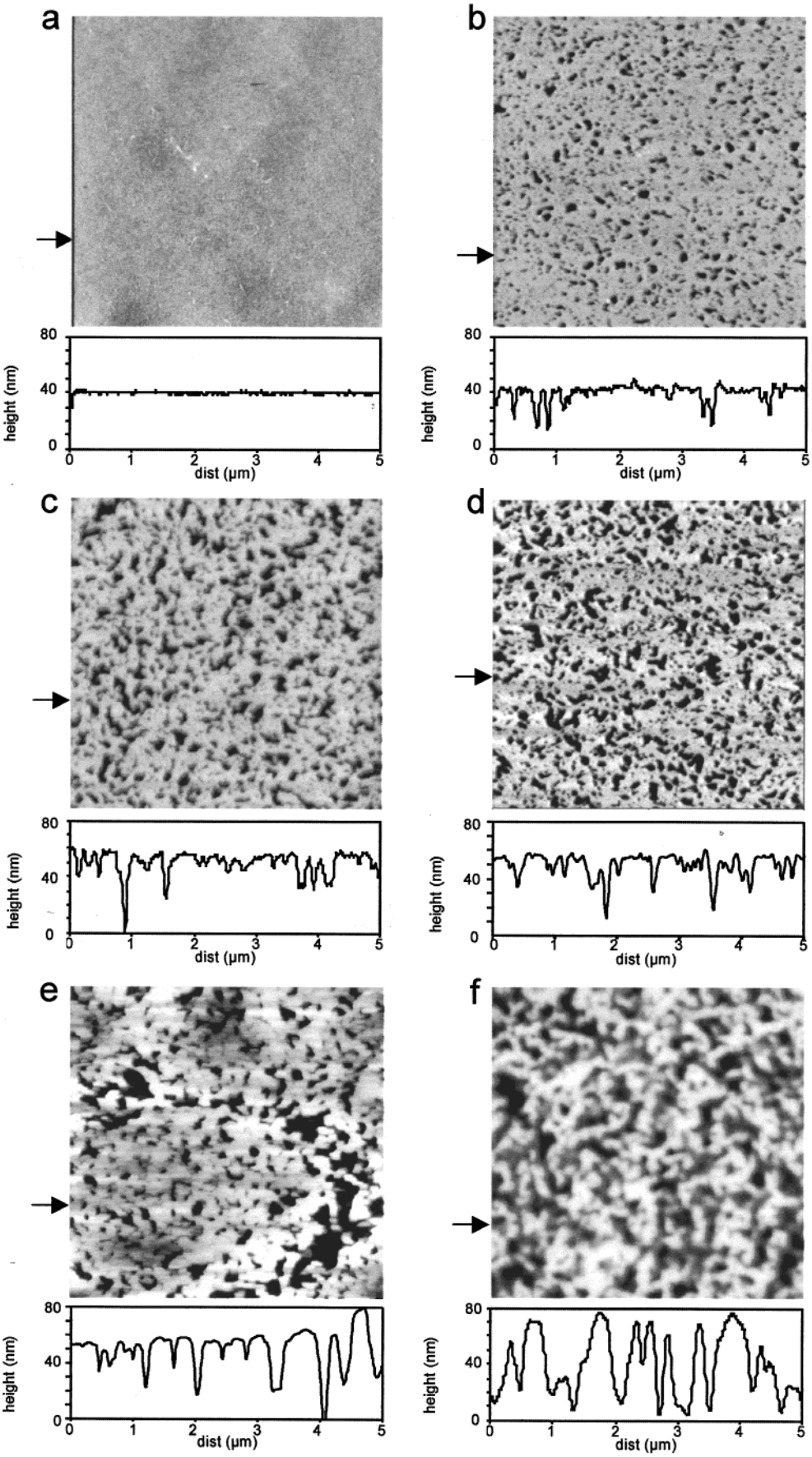

Figure 2. AFM images (size = 5 × 5 μm^2) of samples prepared by collagen adsorption and fast drying (a; *z*-range = 10 nm) and of the same after spin-coating with a PMMA solution at concentration of 0.0 (b; *z*-range = 50 nm), 0.2 (c; *z*-range = 50 nm), 0.5 (d; *z*-range = 50 nm), 1.0 (e; *z*-range = 50 nm), and 2.0 g/L (f; *z*-range = 100 nm). A cross-section taken along the horizontal line indicated by the arrow is shown beneath each image.

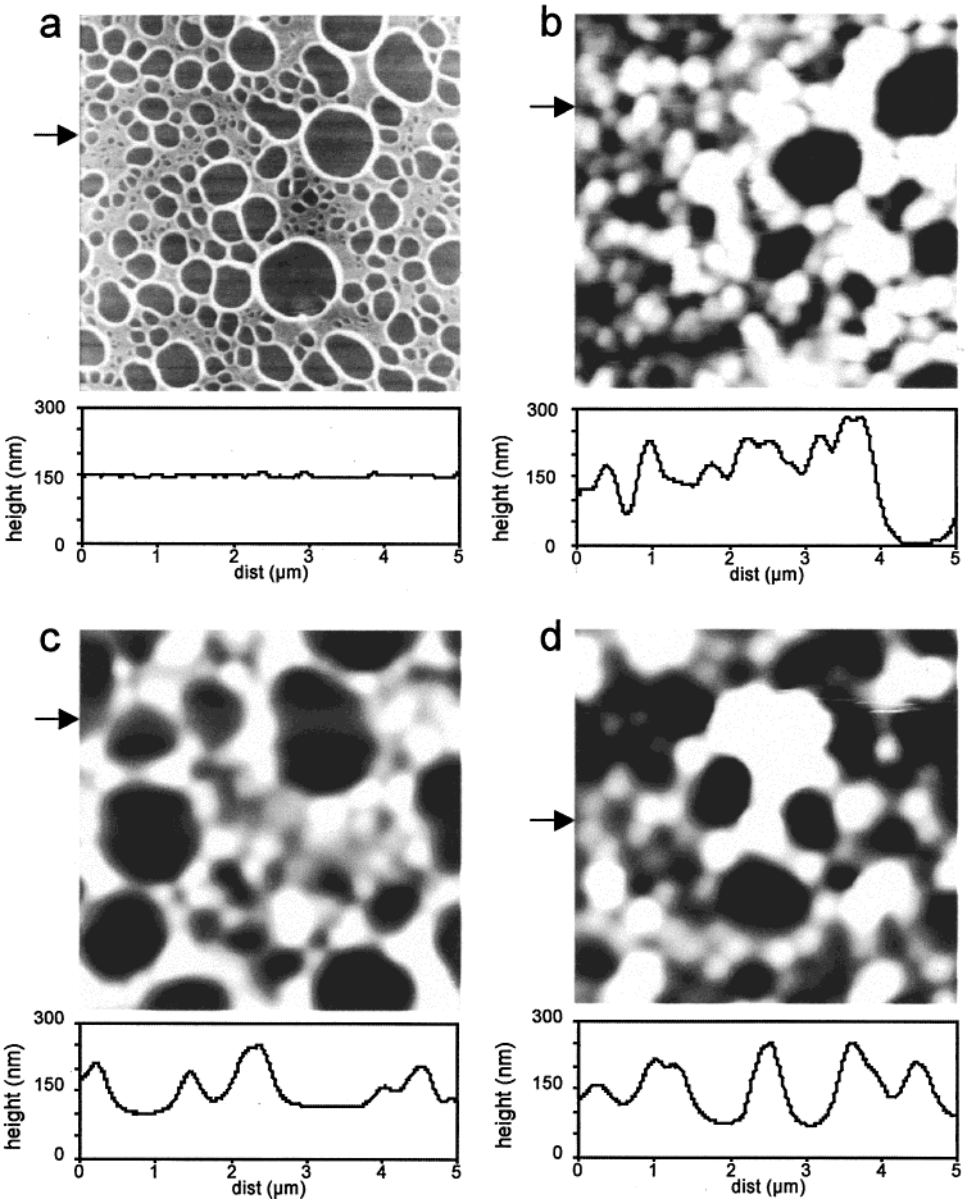

Figure 3. AFM images (size = 5 × 5 μm^2) of samples prepared by collagen adsorption and slow drying (a; *z*-range = 10 nm) and of the same after spin-coating with a PMMA solution at concentration of 0.0 (b; *z*-range = 100 nm), 0.2 (c; *z*-range = 100 nm), and 2.0 g/L (d; *z*-range = 100 nm). A cross-section taken along the horizontal line indicated by the arrow is shown beneath each image.

This is shown in Figure 4a for samples dried at high rates and in Figure 4b for samples dried at low rates after collagen adsorption. The R_{rms} of PMMA was low and increased only slightly and monotonically with the length scale. Adsorption of collagen followed by fast drying (Figure 4a) increased only slightly the R_{rms} compared to PMMA; R_{rms} did not vary appreciably with the length scale. After spin-coating with chlorobenzene, the R_{rms} was much higher and increased up to a length scale of about 300 nm, which corresponded to the size of the holes present at the sample surface. Spin-coating with a 2.0 g/L PMMA solution rendered the R_{rms} even higher at high length scales due to the observed aggregates. However, the variation of R_{rms} at length scales below 300 nm followed that of the samples prepared by spin-coating with pure chlorobenzene, showing that the lateral size of the surface features was in the same range. These trends were reproducible; however, appreciable variations were found between samples prepared in the same conditions. For the sake of clarity, the data presented in Figure 4a were extracted from Figure 2 (images a, b, and f).

The surface pattern obtained after collagen adsorption and slow drying (Figure 4b) led to a significantly higher R_{rms} at high length scale compared to the starting substratum; R_{rms} increased markedly up to a length scale of about 300 nm. Spin-coating still considerably increased the R_{rms}, which rose at length scales between 0.1 and 1 μm. The profile of R_{rms} as a function of the length scale was similar for spin-coating with chlorobenzene and with a 2.0 g/L PMMA solution, showing that the effect of the solvent overwhelmed the effect of the spin-coated polymer. The small confidence intervals shown in Figure 4b indicate that the characteristics of the adsorbed collagen layer and of the relief obtained by subsequent spin-coating with chlorobenzene or PMMA solution are quite reproducible.

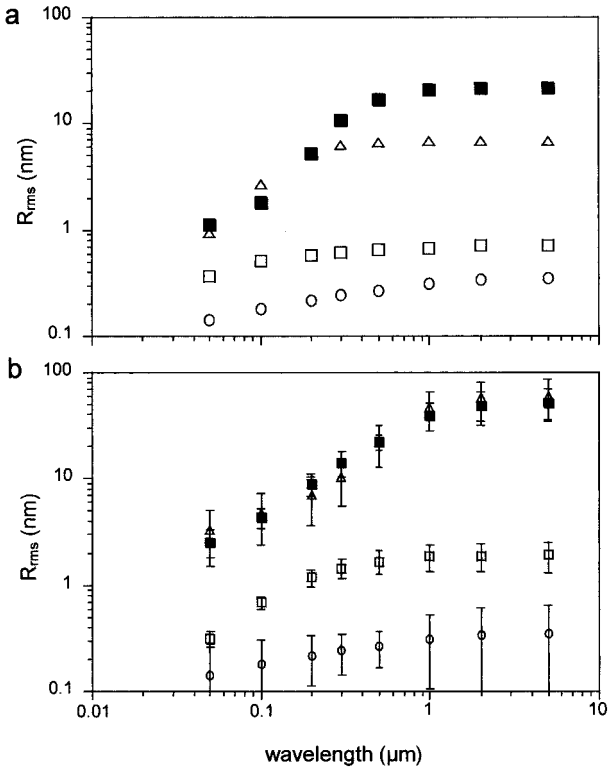

Figure 4. Variation of the R_{rms} as a function of the wavelength for the PMMA substrate after PBS conditioning (○), for the PMMA substrate after collagen adsorption (□), and for the same after spin-coating with chlorobenzene (△) or with a 2.0 g/L PMMA solution (■). (a) Fast drying after collagen adsorption. The confidence intervals obtained from different sets of samples being rather large, the presented data were extracted from the images shown in Figure 2a,b,f, for the sake of clarity. (b) Slow drying after collagen adsorption. The error bars show the confidence interval at 95% (at least two sets of data containing at least three images).

4. Discussion. The surface organization obtained here after adsorption of collagen is in agreement with a previous study:[25] a continuous collagen layer was observed after fast drying, while a discontinuous, patterned collagen layer was obtained by slow drying. The N/C ratio of 0.123 (Table 1) obtained here after fast drying is in agreement with the value of 0.13 found before. Modeling the adsorbed layer as a film of constant thickness (parameters used: concentrations $C_{C,PMMA}$ =59.5 mmol/cm^3, $C_{C,collagen}$ = 56.9 mmol/cm^3, $C_{N,collagen}$ = 19.7 mmol/cm^3 (calculated from the collagen sequence); electron mean free paths $\lambda_{C,PMMA}$ = 3.25 nm,[36] $\lambda_{C,protein}$ = 3.5 nm, $\lambda_{N,protein}$ = 3.2 nm[38]) led to an apparent thickness of about 1 nm. In the previous work, the patterned surface produced at low drying rates was shown to be a net, with holes of a diameter of about 100 nm: PMMA was demonstrated to be exposed at the outermost surface in the holes left by the collagen net. In the work presented here, the main trends are reproduced; however, the collagen layer obtained after slow drying resembles a layer with holes and thick rims (Figure 3a), rather than a net. This difference is attributed to small variations in the kinetics of dewetting.[39]

Here, different surface patterns have been obtained on a PMMA substrate, at the nanometer scale, by spin-coating with either pure chlorobenzene or PMMA solutions subsequently to collagen adsorption. The role of the adsorbed layer on the pattern formation is essential as no comparable topographical changes were observed upon spin-coating on the PMMA substrate (Figure 1).

Spin-coating with pure chlorobenzene on the discontinuous collagen layer obtained by slow drying (Figure 3, Figure 4b) led to a surface topography laterally similar to that of the initial collagen layer, but with much higher and thicker walls. Collagen was no longer detected at the surface (Table 1). This indicates that the PMMA substrate exposed in the holes was dissolved and redeposited on top of the collagen areas, which served as a template. Spin-coating of PMMA solutions of increasing concentrations did not modify the surface relief significantly compared to that obtained with the pure solvent. The dissolution of the PMMA substrate thus overwhelmed the effect of PMMA deposition from the spin-coating solution, the amount of PMMA brought by the solution being negligible compared to that dissolved from the substrate. The solutions of 0.2−2.0 g/L indeed allowed the deposition of 1−5 nm-thick PMMA layers on silicon, while the surface relief obtained here was 10−100 times higher. Spin-coating with a solvent of the substrate is sufficient to obtain chemically homogeneous PMMA surfaces presenting a surface roughness controlled by the organization of the previously adsorbed and slowly dried collagen layer.

Spin-coating with pure chlorobenzene on the smooth collagen layer obtained by fast drying provoked the apparition of holes in the layer (Figure 2b), but the N/C atomic concentration ratio remained practically unchanged (Table 1). As compared with samples covered by a discontinuous collagen layer (slow drying), the thin but dense collagen layer obtained by fast drying limited PMMA dissolution. However, restructuration of the 1 nm thick collagen layer alone may not account for the observed hole formation. Considering the surface occupancy by the holes (23%), this would indeed have produced holes of a depth of 1.3 nm, while 8−40 times deeper holes were observed. The holes were thus formed by pit dissolution of the underlying PMMA. Redeposition of dissolved PMMA was not in the form of a homogeneous film; if this were the case, the N/C ratio would have been reduced at least by a factor of 5, in contrast with the experimental value (Table 1).

Spin-coating with PMMA solutions of increasing concentrations on the smooth collagen layer progressively increased the surface relief compared to the one obtained with the pure solvent (Figure 2). The surface pattern obtained at a PMMA concentration of 2.0 g/L may not be formed by PMMA particles (about 63% of surface coverage) on a collagen layer. If this was the case, the N/C ratio would reach 0.05, while it was found equal to 0.01 (Table 1). Neither may the observed particles be made of collagen: the original collagen layer should indeed have a thickness of at least 20 nm to form such aggregates, and the resulting N/C ratio should be as high as $0.63 \times 0.32 = 0.20$ (0.32 is the N/C ratio expected for pure collagen; the carbon concentration is similar in collagen and PMMA). Moreover, the deposited PMMA layer brought by spin-coating, which is equivalent to a thickness of about 5 nm as observed on silicon, cannot account for

the formation of particles with a 30−80 nm size. The observed surface organization thus results from the combination of dissolution of PMMA from the substrate through the collagen layer and deposition of PMMA by spin-coating; collagen is included in PMMA particles, which results in the weak, but not zero, N/C ratio.

While spin-coating is often used to planarize surfaces, it was shown here that it also allows producing nanometer-scale surface features. Planarization is favored by deposition of a thick polymer layer, using a solvent with low volatility and a low-molar-mass polymer.[29,31] Apart from the solvent (chlorobenzene has a rather low volatility), the conditions chosen here were more favorable to structure formation: the PMMA had a very high molar mass; the concentration of the polymer solutions were very low (0.2−2.0 g/L) compared to those used for planarization (40−100 g/L), leading to deposition of a very thin layer. Moreover, dissolution of the substrate PMMA was either governing or contributing to the relief formation, which was not envisaged in other studies.

5. Conclusion. Different surface patterns were obtained, at the nanometer scale, by spin-coating chlorobenzene or PMMA solutions on collagen layers adsorbed on PMMA substrates. Dissolution of PMMA from the substrate was shown to be a major factor in structure formation. However, the surface architecture (topography and chemical composition) depended on the collagen layer organization. In the case of the discontinuous collagen layer obtained by slow drying, redeposition of PMMA dissolved by chlorobenzene produced a chemically homogeneous surface with cavities in the range 0.1−1 μm diameter and 50−250 nm depth, which resulted from the organization of the initial collagen layer, acting as a template. The PMMA concentration of the spin-coating solution was not an important factor. In the case of the smooth collagen layer obtained by fast drying, the surface organization resulted from a combination of dissolution of PMMA from the substrate and deposition of PMMA by spin-coating. Depending on the PMMA concentration of the spin-coating solution, different structures were obtained, from a pitted collagen layer to a PMMA surface covered by particles of PMMA incorporating collagen.

Different surface architectures, in terms of topography and chemical composition, could now be produced by changing the polymer substrate, playing with the adsorbed compound and its organization, choosing another solvent, modifying the spin-coating parameters, ...

Acknowledgment. We thank P. Grange and P. Bertrand for the use of the atomic force microscope and of the spin-coater, respectively, M. Genet for technical assistance with the XPS measurements, and A.-M. Misselyn-Bauduin for fruitful discussions. The support of the National Foundation for Scientific Research (F.N.R.S.), of the Federal Office for Scientific, Technical and Cultural Affairs (Interuniversity Poles of Attraction Program) and of the Research Department of Communauté Française de Belgique (Concerted Research Action) are gratefully acknowledged.

References

(1) Wennerberg, A.; Albrektsson, T.; Andersson, B. *J. Mater. Sci. Mater. Med* **1995**, *6*, 302.
(2) Hopp, B.; Csete, M.; Révész, K., Vinko, J.; Bor, Zs. *Appl. Surf. Sci.* **1996**, *96−98*, 611.
(3) Miyaki, M.; Fujimoto, K.; Kawaguchi, H. *Colloids Surf. A* **1999**, *153*, 603.
(4) Torimitsu, K.; Kawana, A. *Dev. Brain Res.* **1990**, *51*, 128.
(5) Ito, Y.; Chen, G.; Guan, Y., Imanishi, Y. *Langmuir* **1997**, *13*, 2756.
(6) Jackman, R. J.; Duffy, D. C.; Cherniavskaya, O.; Whitesides, G. M. *Langmuir* **1999**, *15*, 2973.
(7) Walboomers, X. F.; Croes, H. J. E.; Ginsel, L. A.; Jansen, J. A. *J. Biomed. Mater. Res.* **1999**, *47*, 204.
(8) Kumar, A.; Whitesides, G. M. *Science* **1994**, *263*, 60.
(9) Imabayashi, S. I.; Gon, N.; Sasaki, T.; Hobara, D.; Kakiuchi, T. *Langmuir* **1998**, *14*, 2348.
(10) Xu, S.; Liu, G. Y. *Langmuir* **1997**, *13*, 127.
(11) Hiroshima, H.; Komuro, M. *Jpn. J. Appl. Phys.* **1993**, *32*, 6253.
(12) Chou, S. Y.; Krauss, P. R.; Renstrom, P. J. *Science* **1996**, *272*, 85.
(13) Burmeister, F.; Badowsky, W.; Braun, T.; Wieprich, S.; Boneberg, J.; Leiderer, P. *Appl. Surf. Sci.* **1999**, *145*, 461.
(14) Curtis, A.; Wilkinson, C. *Biochem. Soc. Symp.* **1999**, *65*, 15.
(15) Sleytr, U. B.; Sara, M. *Trends. Biotechnol.* **1997**, *15*, 20.
(16) Douglas, K.; Devaud, G.; Clark, N. *Science* **1992**, *257*, 642.
(17) Chernoff, E. A. G.; Chernoff, D. A. *J. Vac. Sci. Technol. A* **1992**, *10*, 596.
(18) Dufrêne, Y.; Marchal, T.; Rouxhet, P. G. *Langmuir* **1999**, *15*, 2871.
(19) Baty, A. M.; Leavitt, P. K.; Siedlecki, C. A.; Tyler, B. J.; Suci, P. A.; Marchant, R. E., Geesey, G. G. *Langmuir* **1997**, *13*, 5702.
(20) Mertig, M.; Thiele, U.; Bradt, J.; Leibiger, G.; Pompe, W.; Wendrock, H. *Surf. Interface Anal.* **1997**, *25*, 514.
(21) Dufrêne, Y. F.; Marchal, T. G.; Rouxhet, P. G. *Appl. Surf. Sci.* **1999**, *144−145*, 638.
(22) Baty, A. M.; Suci, P. A.; Tyler, B. J.; Geesey, G. G. *J. Colloid Interface Sci.* **1996**, *177*, 307.
(23) Lestelius, M.; Liedberg, B.; Tengvall, P. *Langmuir* **1997**, *13*, 5900.
(24) Emch, R.; Zenhausern, F.; Jobin, M.; Taborelli, M.; Descouts, P. *Ultramicroscopy* **1992**, *42−44*, 1155.
(25) Dupont-Gillain, C. C.; Nysten, B.; Rouxhet, P. G. *Polym. Int.* **1999**, *48*, 271.
(26) Stillwagon, L. E.; Larson, R. G. *J. Appl. Phys.* **1988**, *63*, 5251.
(27) Stillwagon, L. E.; Larson, R. G. *Phys. Fluids A* **1990**, *2*, 1937.
(28) Gu, J.; Bullwinkel, M. D.; Campbell, G. A. *J. Electrochem. Soc.* **1995**, *142*, 907.
(29) Bullwinkel, M. D.; Gu, J.; Campbell, G. A.; Sukanak, P. C. *J. Electrochem. Soc.* **1995**, *142*, 2389.
(30) Schiltz, A. *Jpn. J. Appl. Phys.* **1995**, *34*, 4185.
(31) Gupta, S. A.; Gupta, R. K. *Ind. Eng. Chem. Res.* **1998**, *37*, 2223.
(32) Wu, P. Y.; Chou, F. C. *J. Electrochem. Soc.* **1999**, *146*, 3819.
(33) Piskin, E. *J. Biomater. Sci. Polym. Ed.* **1994**, *6*, 775.
(34) Beamson, G.; Briggs, D. *High-resolution XPS of organic polymers: the Scienta ESCA300 database*; John Wiley and Sons: Chichester, U.K., 1992.
(35) Mitchell, D. F.; Clark, K. B.; Bardwell, J. A.; Lennard, W. N.; Massoumi, G. R.; Mitchell, I. V. *Surf. Interface Anal.* **1994**, *21*, 44.
(36) Ashley, J. C. *IEEE Trans. Nucl. Sci.* **1980**, *NS-27*, 1454.
(37) Wieland, M.; Hänggi, P.; Hotz, W.; Textor, M.; Keller, B. A.; Spencer, N. D. *Wear* **2000**, *237*, 231.
(38) Dewez, J. L.; Berger, V.; Schneider, Y. J.; Rouxhet, P. G. *J. Colloid Interface Sci.* **1997**, *191*, 1.
(39) Sharma, A.; Reiter, G. *J. Colloid Interface Sci.* **1996**, *178*, 383.

NL010002X